

Journal Pre-proof

Pracinostat (SB939), a histone deacetylase inhibitor, suppresses breast cancer metastasis and growth by inactivating the IL-6/STAT3 signalling pathways

Jing Chen, Na Li, Boxia Liu, Jun Ling, Wenjun Yang, Xiufeng Pang, Tao Li



PII: S0024-3205(20)30217-4

DOI: <https://doi.org/10.1016/j.lfs.2020.117469>

Reference: LFS 117469

To appear in: *Life Sciences*

Received date: 27 November 2019

Revised date: 8 February 2020

Accepted date: 24 February 2020

Please cite this article as: J. Chen, N. Li, B. Liu, et al., Pracinostat (SB939), a histone deacetylase inhibitor, suppresses breast cancer metastasis and growth by inactivating the IL-6/STAT3 signalling pathways, *Life Sciences*(2020), <https://doi.org/10.1016/j.lfs.2020.117469>

This is a PDF file of an article that has undergone enhancements after acceptance, such as the addition of a cover page and metadata, and formatting for readability, but it is not yet the definitive version of record. This version will undergo additional copyediting, typesetting and review before it is published in its final form, but we are providing this version to give early visibility of the article. Please note that, during the production process, errors may be discovered which could affect the content, and all legal disclaimers that apply to the journal pertain.

© 2020 Published by Elsevier.

**Pracinostat (SB939), a histone deacetylase inhibitor, suppresses
breast cancer metastasis and growth by inactivating the IL-6/STAT3
signalling pathways**

Jing Chen^{a,b,#}, Na Li^{a,b,c,#}, Boxia Liu^{a,b}, Jun Ling^{a,b}, Wenjun Yang^{a,b*}, Xiufeng Pang^{d*},
Tao Li^{e*}

^a School of Basic Medical Sciences, Ningxia Medical University, Yinchuan 750004, China; ^b Key Laboratory of Fertility Preservation and Maintenance (Ningxia Medical University), Ministry of Education, Yinchuan 750004, China; ^c Center for neurological diseases, the first people's hospital of Shizuishan, Shizuishan 753200, China; ^d Shanghai Key Laboratory of Regulatory Biology, Institute of Biomedical Sciences and School of Life Sciences, East China Normal University, Shanghai 200241, China; ^e Department of Oncology, General Hospital of the Ningxia Medical University, Yinchuan 750004, China;

Running title: SB939 suppresses tumor metastasis and tumor growth.

Keywords: HDACs, SB939, breast cancer, EMT, tumor metastasis

The first two authors contributed equally to this work.

*** To whom correspondence should be addressed:**

Dr. Tao Li, and Dr. Wenjun Yang

Department of Oncology, General Hospital of the Ningxia Medical University
1160 Shengli Road, Yinchuan 750004, China.

Phone: +86-51-6980041;

Fax: +86-51-6980041;

E-mail: lit1979@163.com

Dr. Xiufeng Pang

Institute of Biomedical Sciences and School of Life Sciences
East China Normal University

500 Dongchuan Rd.

Shanghai 200241, China

Phone: +86-21-24206942

Fax: +86-21-54344922

E-mail: xfpang@bio.ecnu.edu.cn

Abstract

Aims: Histone deacetylases inhibitors have shown favorable antitumor activity in clinical investigations. In the present study, we assessed the effects of a novel hydroxamic acid-based HDAC inhibitor, SB939, on breast cancer metastasis and tumor growth and characterized the underlying molecular mechanisms.

Main methods: MTS, Wound-healing, and Transwell chamber invasion assays were used to detect the inhibition effects of SB939 on proliferation, migration, and invasion of breast cancer cells. Western blot, cellular immunofluorescence, and EMSA were used to explore the molecular mechanism of SB939 in suppressing breast cancer metastasis. MDA-MB-231 subcutaneous tumor-bearing model of nude mice and the spontaneous metastasis model of breast cancer were both applied to verify *in vivo* anti-tumor growth and anti-metastatic effects.

Key findings: Our results demonstrated that SB939 at 0.5~1 $\mu\text{mol/L}$ markedly impaired the chemotactic motility of breast cancer cells. SB939 reversed epithelial-mesenchymal transition (EMT) process, as evidenced by upregulation E-cadherin expression and downregulation expressions of N-cadherin and vimentin through increasing the levels of ac-histone H3 and H4 and decreasing the expressions of HDAC 5 and 4. This cascade inhibition mediated by SB939 was well interpreted by inactivating phosphorylation of STAT3, blocking its DNA-binding activity, and decreasing the expressions of STAT3-dependent target genes, including MMP2 and MMP9. Furthermore, we found that SB939 significantly inhibited breast cancer metastasis and tumor growth *in vivo* and showed superior anti-tumor properties compared with SAHA in two breast cancer animal models.

Significance: Our findings indicate that SB939 may be an effective therapeutic option for treating advanced breast cancer.

Keywords: HDACs, SB939, breast cancer, EMT, tumor metastasis

Introduction

Worldwide, approximately 2.1 million new female breast cancer cases were diagnosed in 2018, accounting for almost 11.6% of all cancer cases. The disease is the most commonly diagnosed cancer and is the leading cause of cancer death [1]. Breast cancer is a complex heterogeneous disease, and its occurrence and development are biological processes with multiple factors [2].

The majority of breast cancer mortality is due to the development of metastases at distant sites [3]. During metastasis, tumor cells undergo epithelial-to-mesenchymal transition (EMT), a process by which epithelial cells lose their cell-cell adhesion properties and polarity and acquire a migratory and invasive mesenchymal phenotype [4]. Mounting evidence has demonstrated IL-6/STAT3, TGF- β /SMAD, Wnt, and Notch signalling pathways are involved in this process in breast cancer [5-7].

Accumulating evidence has indicated that epigenetic changes play essential roles in the development of breast cancer [8]. Histone acetyltransferases (HATs) and histone deacetylases (HDACs) are necessary enzymes that regulate the dynamic balance of histone acetylation and deacetylation. Dysregulation of histone acetylation and deacetylation is associated with cancer progression. Aberrant HDAC expression has been linked to various cancer types, including breast cancer, gastric cancer, and acute myeloid leukemia [9,10]. Histone deacetylase inhibitors (HDACi) are a group of potent epigenetic drugs that structurally diversified, inhibits HDACs, increase histone acetylation and thereby alter gene transcription. In single agent or combined with traditional chemotherapeutics exerted anti-neoplastic characteristics through cell-cycle arrest, inhibition of migration and invasion, induction of differentiation and apoptosis in many types of cancer cells [11-13]. Based on their chemical structure, four classes of HDACis have been identified, including short-chain fatty acids, hydroxamates, benzamides, and cyclictetrapeptides. The short-chain fatty acid sodium butyrate, the hydroxamic acid trichostatin A and suberoylanilide hydroxamic acid, and other compounds from structurally different families, such as LBH589, valproic acid, and MS-275, have shown favorable antitumor activity with low toxicity in

clinical investigations [9]. Currently, several HDACis are being used as single agent or combined with traditional chemotherapeutics in clinical trials for metastatic breast cancer [14-16]. However, the molecular mechanisms for the anti-cancer activity of HDIs have not been fully resolved.

Pracinostat (SB939), a novel oral, hydroxamic acid-based HDACi, acting on class I, II, and IV HDACs has better pharmacokinetic, physicochemical, and pharmaceutical properties than other inhibitors, such as vorinostat (SAHA) [17]. In the previous study, Kim SH et al. revealed that SB939 shows partial efficacy against 4T1Br4 metastasis to brain in breast cancer [18]. However, the other bio-functions and further mechanisms of SB939 against breast cancer have not been reported.

In this study, we demonstrated that SB939 inhibited proliferation, migration, and invasion in multiple human breast cancer cells by IL-6/STAT3-mediated EMT signalling pathways *in vitro* and *in vivo*. Interestingly, SB939 had shown much stronger anti-metastatic activity *in vitro* and *in vivo* than SAHA. Our results indicate that SB939 is a promising anti-metastatic HDACi that can be further optimized as a therapeutic agent for treating breast cancer.

MATERIALS AND METHODS

Chemicals and reagents

SB939 and SAHA were purchased from Selleck Chemicals (Shanghai, China). Both reagents were dissolved in dimethyl sulfoxide (DMSO) as 20 mmol/L stock solutions and stored at -80°C. Matrigel was purchased from Corning Bioscience (Shanghai, China). Antibodies against phospho-STAT3 (Tyr705), acetyl-histone H3, acetyl-histone H4, and HDAC5 and an Epithelial-Mesenchymal Transition Antibody Sampler Kit were purchased from Cell Signalling Technology Inc. Antibodies against HDAC1, HDAC2, HDAC3, and HDAC4 were purchased from Argobio (Shanghai, China). All other reagents were obtained from Sigma-Aldrich (Sigma-Aldrich, Inc., Shanghai, China).

Cell lines and cell culture

The breast cancer cell lines MDA-MB-231 and MCF-7 were purchased from the American Type Culture Collection. T47D, BT549, and MCF-10A cells were a gift from Dr Mingyao Liu (The Institute of Biomedical Sciences and School of Life Sciences, East China Normal University, Shanghai, China). All of these cells were cultured in RPMI-1640 medium or DMEM supplemented with 10% fetal bovine serum and 1% penicillin/streptomycin. Cells were maintained at 37°C in a humidified 5% CO₂ incubator.

Cell growth inhibition assay

An MTS assay was used to determine cell viability, as previously described [19,20]. Breast cancer cells were seeded at a density of 4 to 5 × 10³ cells per well in 96-well plates and incubated overnight at 37°C. Different concentrations of SB939 or SAHA were used to treat the cells for 48 h. Then, 20 µl of MTS solution was added to each well, and the plates were incubated for 1.5-2 h at 37°C. Cell viability was evaluated by measuring the absorbance of each well at 490 nm with a microplate reader (Bio-Red, USA).

Wound healing assay

A wound-healing assay was performed as described previously [19,21]. Breast cancer cells were seeded in 6-well plates. When cancer cells grew to 80% confluence, “wounds” were created with a sterile 200 μ L pipette tip. Next, fresh 5% serum medium or different concentrations of SB939 or SAHA were added. After 24 h of incubation, the cells were fixed with 4% paraformaldehyde. Images of cells were taken using an inverted microscope (TE2000, Nikon, Japan) at 100 \times magnification. Migrated cells were counted manually, and the inhibition percentage was calculated as a percentage of the untreated group (100%). The assay was repeated three times.

Transwell invasion assays

A cell invasion assay was performed, as described previously [22]. A total of 1×10^5 MDA-MB-231 cells in 150 μ L of medium without FBS were added to the upper chamber, and membranes (8 μ m pore size, 6.5 mm diameter, Corning) coated with Matrigel (BD Biosciences), and 600 μ L of medium with 10% FBS were added to the bottom. Different concentrations of SB939 and SAHA were added to both chambers. After 24 h of incubation, the cells that migrated to the bottom of the membrane were fixed with 4% paraformaldehyde and stained with 0.5% crystal violet solution. The migrated cells were counted under an inverted microscope. The experiment was repeated three times.

Three-dimensional (3D) on-top assay

A 3D on-top assay was performed as previously described [19]. Briefly, Matrigel was added to the 48-well plate and left in a CO₂ incubator for 30 min to solidify. MDA-MB-231 cells (2×10^4) were resuspended in 100 μ L of DMEM with 20% Matrigel and SB939 or SAHA and then seeded on the solidified Matrigel. The on-top Matrigel medium was changed every two days. The experiment was repeated independently three times.

Western blotting analysis

Western blot was performed as described previously [19,20]. Cells were lysed with RIPA buffer containing PMSF and proteinase inhibitor. The protein concentrations were determined using a BCA assay kit (Sigma). Denatured proteins were then

separated by 8-12% SDS-PAGE and transferred to PVDF membranes. The membranes were blocked with 5% BSA for 1-2 h and incubated with specific primary antibodies at 4°C overnight. The next day, the membranes were incubated with HRP-conjugated anti-rabbit or anti-mouse secondary antibodies for one hour. The specifically bound antibodies on the layers were detected with an ECL reagent. Three independent experiments were carried out in triplicate.

Electrophoretic mobility shift assay (EMSA)

The DNA binding activity of STAT3 was determined using an Odyssey Infrared STAT3 EMSA Kit (LI-COR Biosciences, Lincoln, NE, USA) according to the manufacturer's instructions. The STAT3 IRDye 700 infrared dye-labeled oligonucleotides were 5'-GATCCTTCTGGGAATTCCTAGATC-3' and 3'-CTAGGAAGACCCTTAAGGATCTAG-5' (boldface indicates the STAT3-binding sites).

Immunofluorescence assay

A total of 5×10^4 MDA-MB-231 cells were seeded onto round glass coverslips in 24-well plates and treated with or without SB939 for 24 h, followed by stimulation with 100 ng/ml IL-6 for four hours. The cells were fixed with methanol, permeabilized with 0.3% Triton X-100, and blocked with 1% BSA. Next, the slides were incubated overnight at 4°C with rabbit anti-E-cadherin, anti-N-cadherin, and mouse anti-STAT3 antibodies. The next day, the cells were incubated with FITC-conjugated goat anti-mouse or anti-rabbit IgG (Abbkine) for one hour. The chamber slides were then mounted with DAPI (Solarbio) for 5-10 min at room temperature. The images were captured using a fluorescence microscope (Leica DM2000, Germany).

Animal models

All animal care and experimental studies were performed according to the guidelines and animal protocols approved by the Institutional Animal Care and Use Committee of Ningxia Medical University. Female BALB/c athymic nude mice (6 ~ 8 weeks) were bred and maintained at the Experimental Animal Center of Ningxia

Medical University.

For the spontaneous metastasis mouse model, MDA-MB-231 cells (3×10^6) were suspended in sterile PBS (100 μ L) and injected into the 4th abdominal mammary fat pad of each BALB/c mouse. On the seventh day, the mice were divided randomly into three groups (n =7 per group) and received oral SB939 (25 mg/kg), SAHA (25 mg/kg) or DMSO + corn oil (control group). Tumor volumes were measured every other day and calculated according to the formula $V=L \times W^2 \times 0.52$, where L and W refer to the length and width, respectively. After 42 days, when tumor volume of control group mice reached 1200 mm³, all mice were sacrificed. The tumors and lungs were excised for further study. Tumor weights were measured, and lung metastasis nodule numbers were counted manually using a dissecting microscope by three individuals who did not have personal biases regarding the current experiment. The lungs were prepared for H&E staining. The tumors were then made for western blotting and immunohistochemistry analyses.

For the subcutaneous tumor-bearing model, MDA-MB-231 cells (3×10^6 cells per mouse) were injected into the axilla of the mice. When tumors reached approximately 100 mm³, the mice were divided randomly into three groups (n = 6) and received oral SB939 (25 mg/kg), SAHA (25 mg/kg) or DMSO + corn oil (control group) every two days. After four weeks of treatment, the mice were sacrificed, and the tumors and major organs were harvested, weighed, and photographed.

Immunohistochemistry (IHC) analysis

Immunohistochemistry analysis was performed as previously reported [23]. Tumor tissues and lungs were excised, fixed, and embedded in paraffin. The sections were stained with anti-Ki-67 and anti-CD31 antibodies. Images were obtained with a Leica microscope (Leica, DM4000b).

H&E staining

H&E staining was performed as previously reported [24]. Lung was fixed and paraffin-embedded, and the sections were subjected to H&E staining.

Statistical analysis

Statistical comparisons between groups were conducted using one-way ANOVA followed by the Dunnett's test. The data are shown as the mean \pm S.D. or mean \pm S.E.M., as indicated in the figure legends. Differences were considered statistically significant when $P < 0.05$.

Results:

SB939 is a broad-spectrum HDACi

Tumor proliferation is one of the critical steps in the progression and development of cancer [25]. We analyzed cell viabilities in different breast cells (MDA-MB-231, MCF-7, T47D, and MCF-10A) by MTS assay. As shown in Figure 1A, SB939 inhibited cell proliferation in three different breast cancer cell lines, and the IC_{50} values of SB939 in MDA-MB-231, MCF-7, and T47D cells were 10.32 $\mu\text{mol/L}$, 30.98 $\mu\text{mol/L}$ and 5.34 $\mu\text{mol/L}$ respectively. It is worth highlighting that SB939 showed less toxicity on MCF-10A cells with IC_{50} values for 81.58 $\mu\text{mol/L}$. Breast cancer cells were more sensitive to SB939 than to human normal breast epithelial cells MCF-10A, and the inhibitory effects of SB939 on cancer cell proliferation were much better than SAHA. MDA-MB-231 cell morphological changes were detected by crystal violet staining (Figure 1B). Our results suggested that SB939 at tested concentrations (0.5~15 $\mu\text{mol/L}$) dose-dependently reduced the cell numbers and altered the cell morphology compared with the control conditions and SAHA. The chemical structure of SB939 is shown in Figure 1C. The acetylation of histones H3 and H4 is a common hallmark of HDAC inhibition [26]. Therefore, we chose the lower drug concentration (0.1~1 $\mu\text{mol/L}$) to determine the effect of SB939 on H3 and H4 acetylation by western blot assay (Figure 1D and Supplemental Figure 1A and B). Compared to SAHA at the higher concentration (2.5~10 $\mu\text{mol/L}$), SB939 at the lower concentration (0.5~1 $\mu\text{mol/L}$) significantly increased the protein levels of acetylated H3 and H4 ($P < 0.01$). Moreover, we studied the effect of SB939 on HDACs expression. As shown in Figure 1E and Supplemental Figure 1C and D, treatment with SB939 (0.5~1 $\mu\text{mol/L}$; $P < 0.001$) decreased the expression of HDACs in a

dose-dependent manner, especially on HDAC5 and HDAC4. The results from the initial assays suggest that SB939 acts as a broad-spectrum HDACi and has potent antitumor activity against breast cancer.

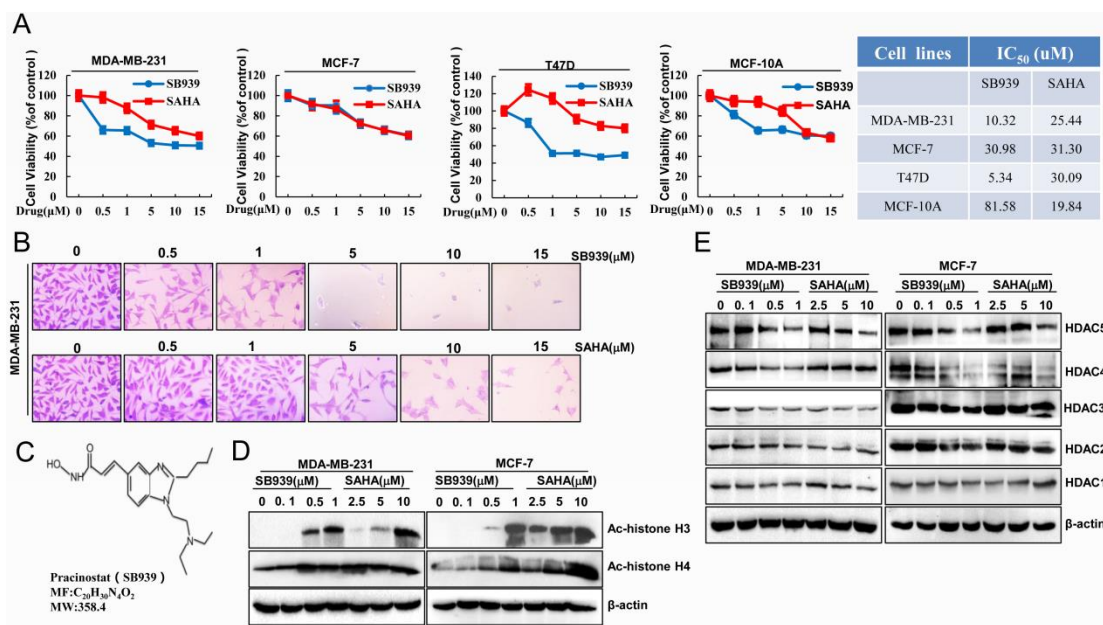


Figure 1. SB939 is a broad-spectrum HDACi. (A) Breast cell lines (MDA-MB-231, MCF-7, T47D, and MCF-10A) were treated with indicated concentrations of SB939 or SAHA. After 48 h, the MTS assay was performed. The bars indicate the mean±SD. (B) crystal violet staining assay was detected MDA-MB-231 cell morphological changes. (C) Chemical structure of SB939. (D) Acetylated histone H3 (Ac-H3) and Acetylated histone H4 (Ac-H4) protein levels were detected by western blot. SAHA was used as a positive control. Actin was used as the loading control. (E) The breast cancer cell line was treated with different concentrations of SB939 or SAHA for 24 h, and then whole-cell lysates were collected. Western blot assays were performed using indicated antibodies.

SB939 has potent metastasis-inhibiting effects on breast cancer cells

Given the importance of tumor cell migration and invasion in the process of tumor metastasis [27], we further evaluated the potential impact of SB939 on breast cancer cell migration. The results showed that treatment with SB939 (0.5~1 μmol/L, $P<0.01$) remarkably impaired the chemotactic motility of breast cancer cells (MDA-MB-231, MCF-7, BT-549, and T47D) in both Wound-healing and Boyden chamber assays (Figure 2 and Figure 3A). The invasive cell numbers of

SB939-treated breast cancer cells was much less than that of the control group and SAHA ($P < 0.01$).

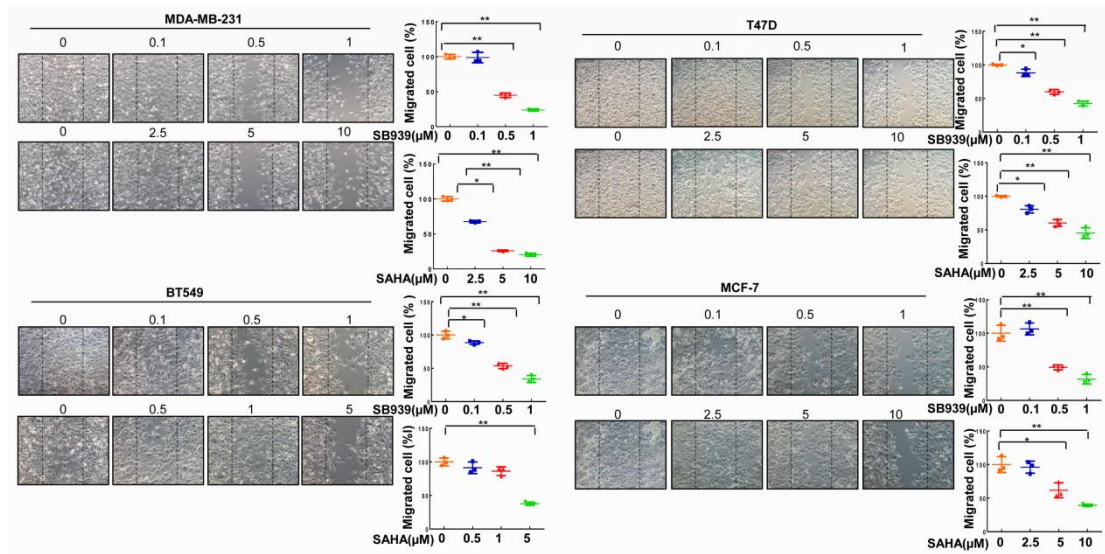


Figure 2. Effects of SB939 on breast cancer migration. SB939 inhibited cell migration in breast cancer cell lines by Wound healing assay. Data were presented as mean \pm s.d, and the significance between different groups was analyzed by One-Way ANOVA. * $P < 0.05$. **, $P < 0.01$ ***, $P < 0.001$.

When highly metastatic breast cancer cells are cultured in 3D matrix glue, they will form irregular clones and "extend" invasive pseudopods into the matrix gel [28]. Therefore, the formation of these pseudopodia partly reflects the infiltration capacity of breast cancer cells. In our three-dimensional cultures, SB939 (0.5~1 $\mu\text{mol/L}$) inhibited MDA-MB-231 chemotactic motility, as few breast cancer cells formed 3D clusters with cells protruding into the surrounding matrix (Figure 3B).

Numerous studies have suggested that EMT is a pivotal step in breast cancer metastasis [9]. To investigate the effect of SB939 on MDA-MB-231 and MCF-7 cell EMT, we performed western blot and immunofluorescence assays. The results showed that SB939 significantly upregulated the expression of E-cadherin while downregulating the expression of N-cadherin, vimentin, and β -catenin (Figure 3C and D and Supplemental Figure 2A and B) with or without IL-6 ($P < 0.001$). Altogether, those data suggested that SB939 shows dose-dependent inhibition effects on breast cancer cell metastases.

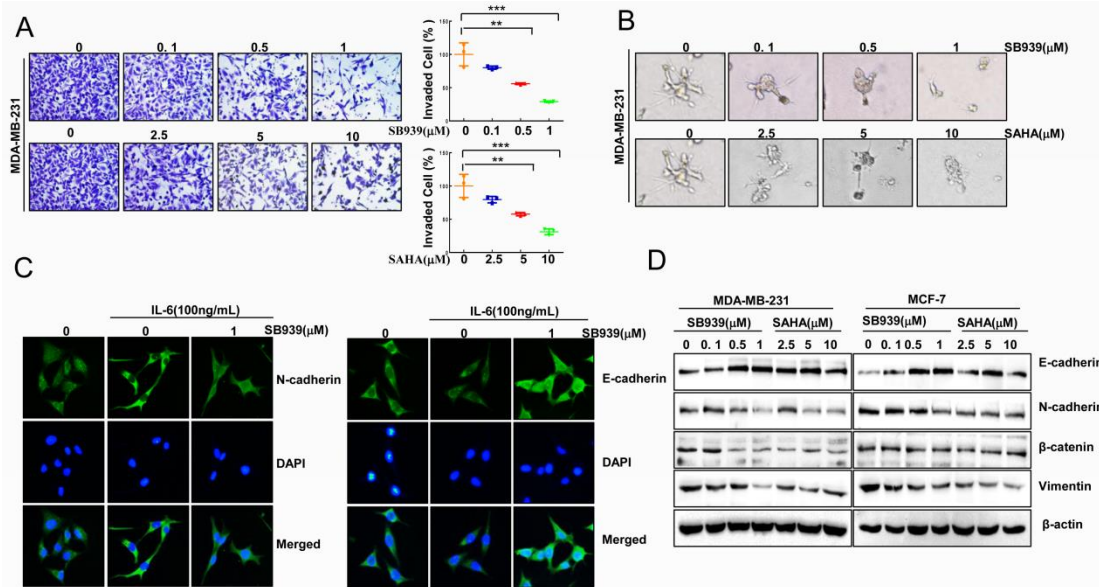


Figure 3. SB939 displays potent tumor metastasis-inhibitory effects on breast cancer cells. (A) SB939 inhibited cell invasion in the MDA-MB-231 breast cancer cell line. The bars indicate the mean \pm SD. Statistically significant differences, **, $P < 0.01$ ***, $P < 0.001$. (B) 3D on-top assay. MDA-MB-231 cells were plated onto indurated Matrigel. After 30 minutes, the DMEM medium containing 20% Matrigel and different concentrations of SB939 or SAHA was added on top of the cells. The Matrigel-medium mixture was replaced every other day. Four days later, cells were photographed. Scale bar, 40 μ m. (C) 5×10^4 MDA-MB-231 cells were seeded on the slider. Cells were treated with SB939 for 24 h and were stimulated with IL-6(100ng/mL) for 4 h, then fixed, and immunofluorescence analysis with the indicated antibodies. Scale bar, 40 μ m. (D) The effect of SB939 on EMT marked protein. Immunoblotting analysis was performed with indicated antibodies.

SB939 inhibits STAT3 signalling and nuclear translocation in breast cancer cells

Signal transducer and activator of transcription 3 (STAT3) is an important transcription factor that is involved in the occurrence and development of malignant tumors [30]. To investigate the effect of SB939 on the constitutive activation of STAT3, MDA-MB-231 and MCF-7 cell lines were treated with SB939 for 24 h and subjected to p-STAT3 immunoblotting. As shown in Figure 4A and Supplemental

Figure 2C and D, SB939 suppressed p-STAT3 expression in a dose-dependent manner but did not affect total STAT3 expression in the cell lines examined ($P < 0.001$). Moreover, we also found that SB939 can suppress the expression of IL-6-induced STAT3 phosphorylation in a dose-dependent manner (Figure 4B and Supplemental Figure 3A and B). The above experiments indicated that SB939 effectively inhibited STAT3 activation. Previous studies demonstrate STAT3 is a transcription factor that must enter the nucleus to be activated. Next, we further evaluated whether SB939 suppressed STAT3 DNA-binding activity and its nuclear translocation by using EMSA and immunofluorescence assays. Our data suggested that treatment with SB939 dose-dependently inhibited the STAT3 DNA binding activity (Figure 4C) and decreased IL-6-induced STAT3 nuclear accumulation (Figure 4D) in MDA-MB-231 cells.

Matrix metalloproteinases (MMPs) also play a key role in tumor invasion and metastasis and are essential target genes downstream of STAT3. Our data showed that SB939 reduced MMP2 and MMP9 expression (Figure 4E and Supplemental Figure 3C and D, $P < 0.01$). These results provide evidence that SB939 specifically inhibits STAT3 tyrosine phosphorylation and decreases the expression of STAT3 downstream target genes by blocking STAT3 DNA binding activity in breast cancer cells.

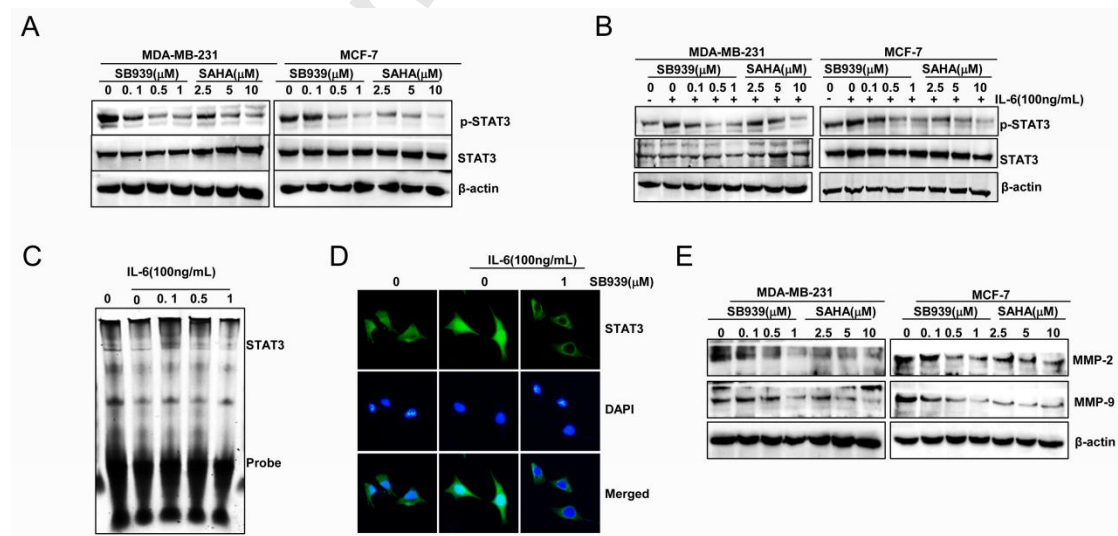


Figure 4. SB939 inhibits STAT3 signaling and nuclear translocation in the breast cancer cells. (A) After treatment with SB939 or SAHA for 24 h, cell extracts were prepared and applied

to immunoblotting with phospho-STAT3 (Tyr-705). β - Actin was used as a loading control. (B) Western blot detected that treatment with SB939 inhibited STAT3 phosphorylation (Tyr-705) with or without IL-6 induction in MDA-MB-231 and MCF-7 cells. (C) MDA-MB-231 cells were treated with different concentrations of SB939. EMSA assay was performed to analyze STAT3 DNA-binding activity. (D) Immunofluorescence analysis of STAT3. MDA-MB-231 cells were treated with various levels of SB939 for 24 h, stained for STAT3(green), and nuclei were stained with DAPI (blue), then observed using a LEICA fluorescence microscope. Scale bar, 40 μ m. (E) Breast cancer cells were pretreated with SB939 for 24 h. Cells were then lysed and applied to immunoblotting with indicated antibodies. Actin was used as a loading control.

SB939 inhibits tumor growth and metastasis in a mouse orthotopic implantation model

To confirm our *in vitro* observations, we established a spontaneous metastasis model of the mammary fat pads of female BALB/c nude mice with one highly aggressive human breast cancer cell line MDA-MB-231. When tumors formed, the nude mice were randomized to receive either control (DMSO+cornoil), SB939 (25 mg/kg), or SAHA (25 mg/kg) orally every other day. The used dosage of SB939 was chosen according to published literature[31-33]. After 42 days, when tumor volume of control group mice reached 1200mm³, all mice were executed. As presented in Figure 5A, B, and C, we found that mice treated with SB939 had significantly smaller tumor volumes and weights than the control group and SAHA treatment group ($P < 0.01$). On the 42 day, all mice were executed, and their lungs were removed. As shown in Figure 5 D and E, the numbers of lung metastasis nodules were fewer in the SB939 treatment group than in the control and SAHA treatment groups ($P < 0.01$). Notably, Western blot analysis showed that the acetylation levels of histone H3 and H4 ($P < 0.001$) in the tumor tissues were increased in both SB939 and SAHA-treated groups (Figure 5F and Supplemental Figure 4A and B). At the same dose, the acetylation levels of histone H3 and H4 in the SB939-treated group were much higher than SAHA, confirming that stronger HDAC inhibitory effect of SB939 on breast cancer *in vivo*. Moreover, we

found that SB939 inhibited phospho-STAT3 activation, E-cadherin and N-cadherin (Figure 5F and Supplemental Figure 4C and D and E). These results are consistent with our *in vitro* results.

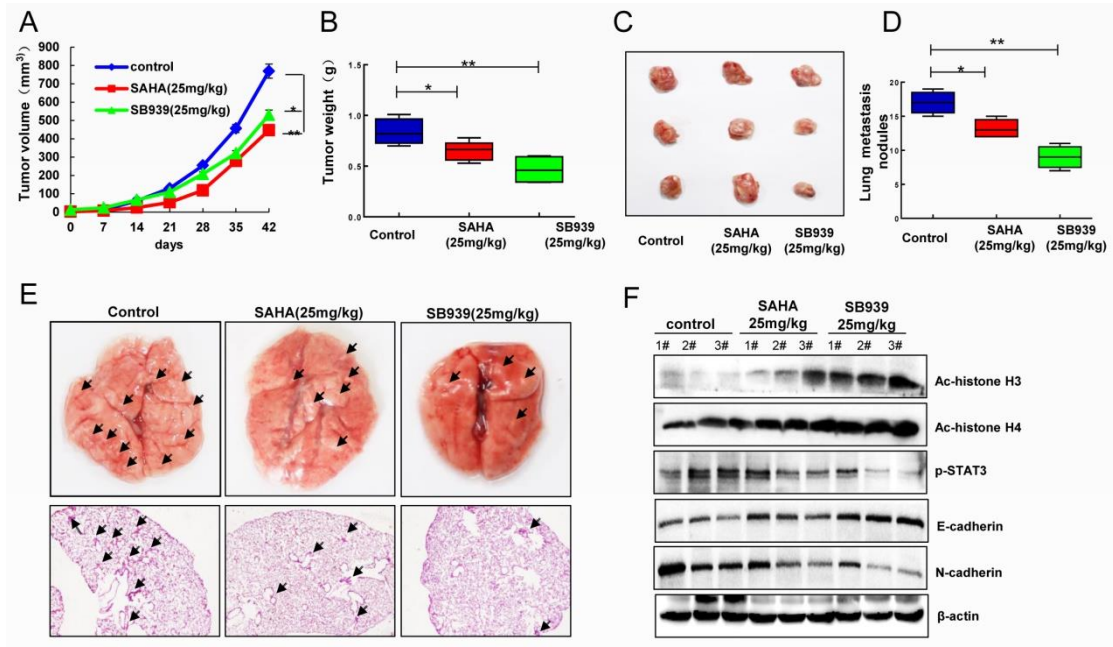


Figure 5. SB939 inhibits tumor growth and metastasis in a spontaneous metastasis model in mice. (A) Tumor volume was measured every other day. Statistically significant differences, * $P < 0.05$, ** $P < 0.01$. (B, C) Tumors' tissue was removed and weighed. Statistically significant differences, * $P < 0.05$, ** $P < 0.01$. (D, E) Lung metastasis nodules were observed, and lung metastasis nodules were counted manually. Statistically significant differences (Student's t-test), * $P < 0.05$, ** $P < 0.01$. (F) Acetylated histone H3 (Ac-H3) and acetylated histone H4 (Ac-H4) protein level, STAT3 phosphorylation E-cadherin and N-cadherin in tumor tissue were detected using western blot analysis.

During treatment, body weights were measured every other day. The body weights of the mice were not significantly changed after treatment (Figure 6A). When the skin of each mouse was pulled back to expose the internal organs, no significant changes in mouse visceral color were found after treatment (Figure 6B). Our results indicated that SB939 caused less toxicity in mice at the test concentrations.

Besides, we found that SB939 suppressed tumor angiogenesis, as shown in Figure 6C. IHC analysis showed that SB939 significantly reduced CD31 and Ki-67 levels *in vivo* (Figure 6D). These results may imply that SB939 showed superior

pharmacodynamic properties compared with SAHA *in vivo*.

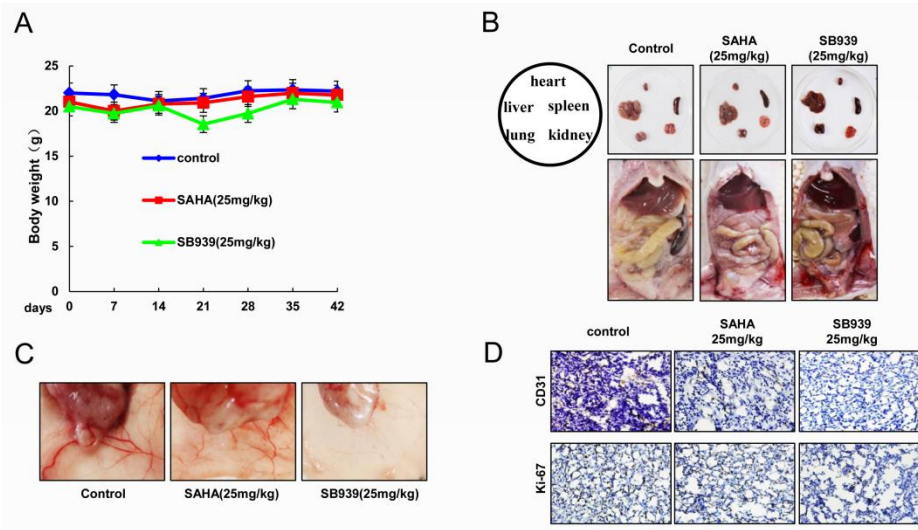


Figure 6. Effects of SB939 on toxicity and angiogenesis in mice. (A) The body weight of control and treated mice were recorded and analyzed once a day. (B) After 42 days of treatment, the image of major organs was shown. (C) Neovascularization was observed after 42 days. (D) IHC staining of CD31 and KI-67 in metastatic lung tumors.

SB939 inhibits tumor growth in a breast cancer subcutaneous tumor model

As SB939 has anti-proliferation and anti-migration effects on different breast cancer cells *in vitro*, we investigated the preliminary anticancer efficacy of SB939 *in vivo*. A BALB/c nude mouse MDA-MB-231 subcutaneous xenograft model was established to investigate antitumor growth activity. Mice were given oral gavages of SB939 (25 mg/kg) or SAHA (25 mg/kg) for 28 days. SB939 significantly inhibited tumor volume (Figure 7A) and weight (Figure 7B and C). The antitumor growth effect of SB939 was better than that of SAHA. The percent tumor growth inhibition (TGI) of SB939 was 50% in the 25 mg/kg group, and that of SAHA was 32% in the 25 mg/kg group. No significant changes in mice body weights (Figure 7D) or organ color (Figure 7E) were observed after SB939 and SAHA treatment. These results suggest that the mice could tolerate the effective doses of SB939. We also found that SB939 treatment was well correlated with angiogenesis inhibition (Figure 7F).

Collectively, these results indicated that the SB939-mediated suppression of breast tumor growth *in vivo* was associated with decreased neovascularization.

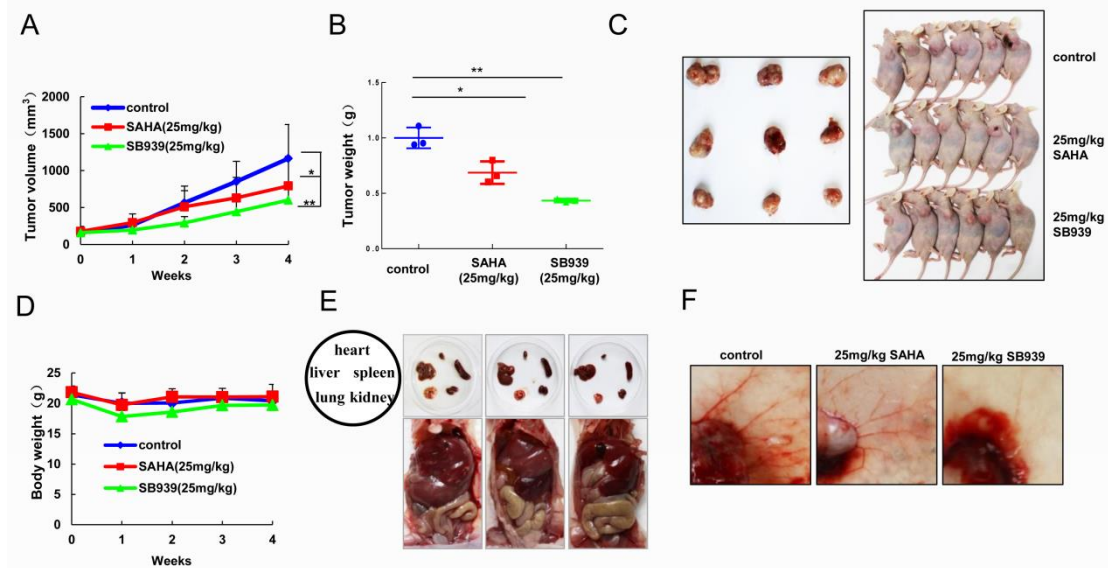


Figure 7. SB939 suppresses tumor growth of mice in a subcutaneous tumor model. (A) SB939 inhibited tumor growth as measured by tumor volume. Statistically significant differences, * $P < 0.05$, ** $P < 0.01$. (B) The cartogram of tumor weight in each group was shown, * $P < 0.05$, ** $P < 0.01$. (C). The image of the tumor tissue in each group was shown. (D) Mice body weight was measured by scales once a day. (E) After four weeks of treatment, the image of major organs was shown, and there was no detectable toxicity. (F) Neovascularization was observed after four weeks.

Discussion

Breast cancer is the second leading cause of cancer death among women worldwide. Currently, increasingly researches have shown that HDACs have become attractive targets in tumor target therapy [34]. However, no HDACi has been approved by the FDA for breast cancer treatment. So far, 62 HDACis have been registered in ClinicalTrials for breast cancer treatment [35]. More importantly, clinical data show that HDACis have good tolerance and limited toxicity in addition to their antitumor activity [36, 37]. In this study, we describe a novel hydroxamic acid-based HDACi, SB939, showed good anti-breast cancer growth and metastasis *in vitro* and *in vivo*.

Although Kim SH et al. Reported that SB939 could significantly inhibit the orthotopic growth of breast tumor brain metastases [18]. But there was further study needed to reveal its bio function and anti-cancer mechanisms. In this study, we showed the crucial findings that a low concentration of SB939 inhibits several characteristics of cancer *in vitro*, including tumor cell migration and invasion. The MTS assay results showed that SB939 inhibited cell proliferation in a dose-dependent manner. In addition, the effect of the tested SB939 on non-tumorigenic human breast epithelial cells MCF-10A was also determined to assess for the cytotoxicity to normal cells. We found that MCF-7, T47D cells, and MDA-MB-231 cells were more sensitive to SB939 than MCF-10A cells. The results indicated SB939 exerted less cytotoxicity. When further comparing the effect of SB939 and SAHA on breast cancer cell migration and invasion, interestingly, SB939 at the lower concentration of 1 μ mol/L was found to inhibit the migration and invasion of breast cancer cells dramatically. We discovered that SB939 significantly increased the acetylation of HDAC-related biomarkers, such as histones H3 and H4, and inhibited the expressions of HDACs, especially on HDAC5 and HDAC4. These results suggest that SB939 is a broad-spectrum pan-HDACi and that SB939 has stronger anti-metastatic activity than

SAHA.

EMT plays a crucial step in the tumor invasion and metastasis process and includes a common molecular mechanism of tumor metastasis [38-39]. During EMT, epithelial cells lose their cell polarity and cell-cell adhesion; ultimately, they become mesenchymal cells and acquire migration and invasion properties, which are characterized by intercellular adhesion loss, epithelial cell marker protein downregulation and mesenchymal cell marker upregulation [40]. Recent reports indicate that the IL-6/JAK/STAT3 pathway plays a pivotal role in the occurrence and development of breast carcinoma. STAT3, a latent self-signaling transcription factor, is activated by certain interleukins (e.g., IL-6) and growth factors, which can be further activated by non-receptor tyrosine kinase JAK2, and c-Src family kinase. Upon activation, STAT3 undergoes phosphorylation, homodimerization, nuclear translocation, and DNA binding, which subsequently leads to transcription of various target genes involved in regulating cell survival, angiogenesis, metastasis, immune evasion and inflammation in tumor microenvironment [41,42]. To date, 18 HDAC family members have been identified and classified into four groups based on their homology to yeast histone deacetylases: Class I (HDAC1, 2, 3 and 8), Class II (HDAC4, 5, 6, 7, 9 and 10), Class III (SIRT1–7) and Class IV (HDAC11). Studies have shown that the activities of HDAC1 and HDAC2 are directly involved in the negative regulation of STAT3 transcriptional activity [43]. Moreover, other studies have found that HDAC3 knockdown markedly decreases both tyrosine (Y705) and serine (S727) phosphorylation of STAT3 [44]. However, little has been reported that how HDAC4 and HDAC5 affect STAT3 phosphorylation. Only one study has shown that HDAC5 acts directly on STAT3—via reciprocal STAT3 deacetylation at Lys685 and phosphorylation at Tyr705—presents a critical step in STAT3 transcriptional activation and leptin signalling [45]. In this study, we found that SB939 markedly inhibited expressions of HDAC5 and HDAC4. We also investigated the molecular mechanism and found that SB939 markedly inhibited endogenous and IL-6-induced STAT3 phosphorylation in MDA-MB-231 and MCF-7 breast cancer cells, as well as STAT3 transportation into the nucleus, at an adequate concentration of 0.5-1 $\mu\text{mol/L}$

We found that SB939 increased E-cadherin expression and suppressed N-cadherin expression induced by IL-6 by immunofluorescence assay. These results suggested that SB939 might block HDAC5 to act directly on STAT3 and restrain the phosphorylation of STAT3 to reverse EMT progression to suppress breast cancer metastasis. The specific mechanism of how SB939 affects STAT3 phosphorylation through HDAC4 and HDAC5 will be further investigated in our next work..

In the above studies, we found that SB939 can significantly inhibit the invasion and metastasis of breast cancer, and its inhibitory effect was better than that of the positive control drug SAHA. To evaluate the anti-breast cancer growth and metastasis activity of SB939 *in vivo*, we established a spontaneous metastasis model and subcutaneous tumor model in nude mice. In the former one, we found that SB939 (25 mg/kg) can effectively inhibit breast tumor metastasis to the lungs and reduced p-STAT3 expression and increased levels of acetylated histones H3 and H4 in tumor tissues. These results indicate that the bio-functions of SB939 may be target-specific. We also found that SB939 can effectively inhibit breast tumor growth in a tumor-bearing nude mice model. The body weights and visceral color of nude mice were not significantly different between the SB939 treatment group and the control group, indicating that SB939 has low toxicity at this tested concentration. Considering all these findings, SB939 may be a promising candidate for anticancer drugs. However, further investigations are needed to substantiate this hypothesis carefully.

Conclusion

Our results demonstrate that HDAC inhibitor SB939 can inhibit the growth and metastasis of breast cancer *in vitro* and *in vivo*, and its inhibitory effect is superior to that of the positive control drug SAHA. It is also proved that SB939 might block HDAC5 which acts directly on STAT3 to restrain the phosphorylation of STAT3 to reverse EMT progression to suppress breast cancer metastasis. Our study provides a theoretical basis for the treatment of breast cancer.

Fundings

This work is supported by the grants from the National Natural Science Foundation of China (81560485, 816660500, 81760525), West China Top Class Discipline Project in Basic Medical Sciences, Ningxia Medical University (NXYLXK2017B07 and NXYLXK2017A05); and Natural Science Foundation of Ningxia (NZ16142).

Conflicts of interest

The authors declare no conflicts of interest.

Journal Pre-proof

References

- [1] Bray F, Ferlay J, Soerjomataram I, Siegel RL, Torre LA, Jemal A. Global cancer statistics 2018: GLOBOCAN estimates of incidence and mortality worldwide for 36 cancers in 185 countries. *CA Cancer J Clin.* (2018);68:394-424.
- [2] Poorhosseini SM, Hashemi M, Alipour Olyaei N, Izadi A, Moslemi E, Ravesh Z, et al. New Gene Profiling in Determination of Breast Cancer Recurrence and Prognosis in Iranian Women. *Asian Pacific journal of cancer prevention : APJCP.* (2016);17:155-60.
- [3] Weigelt B, Peterse JL, van 't Veer LJ. Breast cancer metastasis: markers and models. *Nat Rev Cancer.* (2005);5:591-602.
- [4] Lamouille S, Xu J, Derynck R. Molecular mechanisms of epithelial-mesenchymal transition. *Nat Rev Mol Cell Biol.* (2014);15:178-96.
- [5] Gyamfi J, Lee YH, Eom M, Choi J. Interleukin-6/STAT3 signalling regulates adipocyte induced epithelial-mesenchymal transition in breast cancer cells. *Sci Rep.* (2018);8:8859.
- [6] Lv ZD, Kong B, Li JG, Qu HL, Wang XG, Cao WH, Liu, X. Y. Wang, Y. Yang, Z. C. Xu, H. M. Wang, H. B. Transforming growth factor-beta 1 enhances the invasiveness of breast cancer cells by inducing a Smad2-dependent

- epithelial-to-mesenchymal transition. *Oncol Rep.* (2013);29:219-25.
- [7] Kotiyal S, Bhattacharya S. Breast cancer stem cells, EMT and therapeutic targets. *Biochem Biophys Res Commun.* (2014);453:112-6.
- [8] Huang Y, Nayak S, Jankowitz R, Davidson NE, Oesterreich S. Epigenetics in breast cancer: what's new? *Breast Cancer Res.* (2011);13:225.
- [9] West AC, Johnstone RW. New and emerging HDAC inhibitors for cancer treatment. *J Clin Invest.* (2014);124:30-9.
- [10] Li Y, Seto E. HDACs, and HDAC Inhibitors in Cancer Development and Therapy. *Cold Spring Harb Perspect Med.* (2016);6.
- [11] The anticancer effects of MPT0G211, a novel HDAC6 inhibitor, combined with chemotherapeutic agents in human acute leukemia cells. *Clinical epigenetics.* (2018);10:162.
- [12] Piao J, Chen L, Quan T, Li L, Quan C, Piao Y, et al. Superior efficacy of co-treatment with the dual PI3K/mTOR inhibitor BEZ235 and histone deacetylase inhibitor Trichostatin A against NSCLC. *Oncotarget.* (2016);7:60169-80.
- [13] Eckschlager T, Plch J, Stiborova M, Hrabeta J. Histone Deacetylase Inhibitors as Anticancer Drugs. *International journal of molecular sciences.* (2017);18.
- [14] Srivastava RK, Kurzrock R, Shankar S. MS-275 sensitizes TRAIL-resistant breast cancer cells, inhibits angiogenesis and metastasis, and reverses epithelial-mesenchymal transition in vivo. *Mol Cancer Ther.* (2010);9:3254-66.
- [15] Liu Y, Liggitt D, Fong S, Debs RJ. Systemic co-administration of depsipeptide selectively targets transfection enhancement to specific tissues and cell types. *Gene*

Ther. (2006);13:1724-30.

[16] Munster PN, Thurn KT, Thomas S, Raha P, Lacevic M, Miller A, Melisko, M. Ismail-Khan, R. Rugo, H. Moasser, M. Minton, S. E. A phase II study of the histone deacetylase inhibitor vorinostat combined with tamoxifen for the treatment of patients with hormone therapy-resistant breast cancer. *Br J Cancer*. (2011);104:1828-35.

[17] Novotny-Diermayr V, Sangthongpitag K, Hu CY, Wu X, Sausgruber N, Yeo P, Greicius, G. Pettersson, S.Liang, A. L. Loh, Y. K. Bonday, Z. Goh, K. C. Hentze, H. Hart, S. Wang, H. Ethirajulu, K. Wood, J. M.SB939, a novel potent and orally active histone deacetylase inhibitor with high tumor exposure and efficacy in mouse models of colorectal cancer. *Mol Cancer Ther*. (2010);9:642-52.

[18] Kim SH, Redvers RP, Chi LH, Ling X, Lucke AJ, Reid RC, Fairlie, D. P. Martin, Acbm Anderson, R. L. Denoyer, D. Pouliot, N. Identification of brain metastasis genes and therapeutic evaluation of histone deacetylase inhibitors in a clinically relevant model of breast cancer brain metastasis. *Dis Model Mech*. (2018);11.

[19] Li J, Zhang T, Yang F, He Y, Dai F, Gao D, Chen, Y. Liu, M. Yi, Z. Inhibition of breast cancer progression by a novel histone deacetylase inhibitor, LW479, by down-regulating EGFR expression. *Br J Pharmacol*. (2015);172:3817-30.

[20] Li T, Liu X, Shen Q, Yang W, Huo Z, Liu Q, Jiao, H. Chen, J. Salinomycin exerts anti-angiogenic and anti-tumorigenic activities by inhibiting vascular endothelial growth factor receptor 2-mediated angiogenesis. *Oncotarget*. (2016);7:26580-92.

[21] Zhang T, Li J, Ma X, Yang Y, Sun W, Jin W, Wang, L. He, Y. Yang, F. Yi, Z. Hua, Y. Liu, M. Chen, Y. Cai, Z. Inhibition of HDACs-EphA2 Signaling Axis with WW437

Demonstrates Promising Preclinical Antitumor Activity in Breast Cancer.

EBioMedicine. (2018);31:276-86.

[22] Zhang T, Chen Y, Li J, Yang F, Wu H, Dai F, Hu, M.Lu, X. Peng, Y. Liu, M. Zhao, Y. Yi, Z. Antitumor action of a novel histone deacetylase inhibitor, YF479, in breast cancer. *Neoplasia*. (2014);16:665-77.

[23] Tang X, Shi L, Xie N, Liu Z, Qian M, Meng F, Xu, Q. Zhou, M. Cao, X. Zhu, W. G. Liu, B. SIRT7 antagonizes TGF-beta signaling and inhibits breast cancer metastasis. *Nat Commun*. (2017);8:318.

[24] Zhang T, Li J, Yin F, Lin B, Wang Z, Xu J, Wang, H. Zuo, D. Wang, G. Hua, Y. Cai, Z. Toosendanin demonstrates promising antitumor efficacy in osteosarcoma by targeting STAT3. *Oncogene*. (2017);36:6627-39.

[25] Hainaut P, Plymoth A. Targeting the hallmarks of cancer: towards a rational approach to next-generation cancer therapy. *Curr Opin Oncol*. (2013);25:50-1.

[26] Somech R, Izraeli S, A JS. Histone deacetylase inhibitors--a new tool to treat cancer. *Cancer Treat Rev*. (2004);30:461-72.

[27] Mikula-Pietrasik J, Uruski P, Tykarski A, Ksiazek K. The peritoneal "soil" for a cancerous "seed": a comprehensive review of the pathogenesis of intraperitoneal cancer metastases. *Cell Mol Life Sci*. (2018);75:509-25.

[28] Lu J, Guo H, Treekitkarnmongkol W, Li P, Zhang J, Shi B, Ling, C. Zhou, X. Chen, T. Chiao, P. J. Feng, X. Seewaldt, V. L. Muller, W. J. Sahin, A. Hung, M. C. Yu, D. 14-3-3zeta Cooperates with ErbB2 to promote ductal carcinoma in situ progression to invasive breast cancer by inducing epithelial-mesenchymal transition. *Cancer Cell*.

(2009);16:195-207.

[29] Yeung KT, Yang J. Epithelial-mesenchymal transition in tumor metastasis. *Mol Oncol.* (2017);11:28-39.

[30] Zhang T, Li S, Li J, Yin F, Hua Y, Wang Z, et al. Natural product pectolinarigenin inhibits osteosarcoma growth and metastasis via SHP-1-mediated STAT3 signaling inhibition. *Cell Death Dis.* (2016);7:e2421.

[31] Kim SH, Redvers RP, Chi LH, Ling X, Lucke AJ, Reid RC, Fairlie, D. P. Martin, Acbm Anderson, R. L. Denoyer, D. Pouliot, N. Identification of brain metastasis genes and therapeutic evaluation of histone deacetylase inhibitors in a clinically relevant model of breast cancer brain metastasis. *Dis Model Mech.* (2018);11.

[32] Novotny-Diermayr V, Sangthongpitag K, Hu CY, Wu X, Sausgruber N, Yeo P, et al. SB939, a novel potent and orally active histone deacetylase inhibitor with high tumor exposure and efficacy in mouse models of colorectal cancer. *Mol Cancer Ther.* (2010);9:642-52.

[33] Sooraj D, Xu D, Cain JE, Gold DP, Williams BR. Activating Transcription Factor 3 Expression as a Marker of Response to the Histone Deacetylase Inhibitor Pracinostat. *Mol Cancer Ther.* (2016);15:1726-39.

[34] New M, Olzscha H, La Thangue NB. HDAC inhibitor-based therapies: can we interpret the code? *Mol Oncol.* (2012);6:637-56

[35] Huang M, Zhang J, Yan C, Li X, Zhang J, Ling R. Small molecule HDAC inhibitors: Promising agents for breast cancer treatment. *Bioorg Chem.* (2019);91:103184.

[36] Kelly WK, O'Connor OA, Krug LM, Chiao JH, Heaney M, Curley T, MacGregore-Cortelli, B. Tong, W. Secrist, J. P. Schwartz, L. Richardson, S. Chu, E.

Olgac, S. Marks, P. A. Scher, H. Richon, V. M Phase I study of an oral histone deacetylase inhibitor, suberoylanilide hydroxamic acid, in patients with advanced cancer. *J Clin Oncol.* (2005);23:3923-31.

[37] Goldstein LJ, Zhao F, Wang M, Swaby RF, Sparano JA, Meropol NJ, Bhalla, K. N. Pellegrino, C. M. Katherine Alpaugh, R. Falkson, C. I. Klein, P. Sledge, G. W. A Phase I/II study of suberoylanilide hydroxamic acid (SAHA) in combination with trastuzumab (Herceptin) in patients with advanced metastatic and/or local chest wall recurrent HER2-amplified breast cancer: a trial of the ECOG-ACRIN Cancer Research Group (E1104). *Breast Cancer Res Treat.* (2017);165:375-82.

[38] Wittekind C, Neid M. Cancer invasion and metastasis. *Oncology.* (2005);69 Suppl 1:14-6.

[39] Blick T, Widodo E, Hugo H, Waltham M, Lenburg ME, Neve RM, Thompson, E. W. Epithelial mesenchymal transition traits in human breast cancer cell lines. *Clin Exp Metastasis.* (2008);25:629-42.

[40] Das V, Bhattacharya S, Chikkaputtaiah C, Hazra S, Pal M. The basics of epithelial-mesenchymal transition (EMT): A study from a structure, dynamics, and functional perspective. *J Cell Physiol.* (2019).

[41] Johnson DE, O'Keefe RA, Grandis JR. Targeting the IL-6/JAK/STAT3 signalling axis in cancer. *Nature reviews Clinical oncology.* 2018;15:234-48.

[42] Debnath B, Xu S, Neamati N. Small molecule inhibitors of signal transducer and activator of transcription 3 (Stat3) protein. *Journal of medicinal chemistry.* (2012);55:6645-68.

- [43] Icardi L, Lievens S, Mori R, Piessevaux J, De Cauwer L, De Bosscher K, et al. Opposed regulation of type I IFN-induced STAT3 and ISGF3 transcriptional activities by histone deacetylases (HDACS) 1 and 2. *FASEB journal : official publication of the Federation of American Societies for Experimental Biology*. (2012);26:240-9.
- [44] Minami J, Suzuki R, Mazitschek R, Gorgun G, Ghosh B, Cirstea D, et al. Histone deacetylase 3 as a novel therapeutic target in multiple myeloma. *Leukemia*. (2014);28:680-9.
- [45] Kabra DG, Pfuhlmann K, Garcia-Caceres C, Schriever SC, Casquero Garcia V, Kebede AF, et al. Hypothalamic leptin action is mediated by histone deacetylase 5. *Nature communications*. (2016);7:10782.

Highlights

- EMT plays a key step in the tumour invasion and metastasis process.
- IL-6/STAT3 has been shown to play an important role in inducing the EMT.
- HDACis have become attractive targets for metastatic breast cancer.
- SB939 showed superior anti-metastatic properties compared with SAHA.

Journal Pre-proof